Article

The Molecular Basis of Resilience to the Effect of the Lys103Asn Mutation in Non-Nucleoside HIV-1 Reverse Transcriptase Inhibitors Studied by Targeted Molecular Dynamics Simulations

Ftima Rodrguez-Barrios, Jan Balzarini, and Federico Gago

J. Am. Chem. Soc., **2005**, 127 (20), 7570-7578• DOI: 10.1021/ja042289g • Publication Date (Web): 30 April 2005

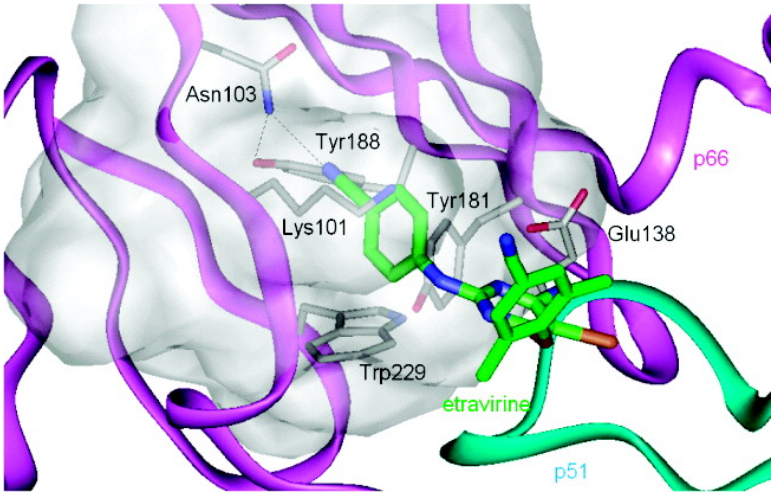

More About This Article

Additional resources and features associated with this article are available within the HTML version:

- Supporting Information
- Links to the 4 articles that cite this article, as of the time of this article download
- Access to high resolution figures
- Links to articles and content related to this article
- Copyright permission to reproduce figures and/or text from this article

View the Full Text HTML

J|A|C|S
ARTICLES
Published on Web 04/30/2005

The Molecular Basis of Resilience to the Effect of the Lys103Asn Mutation in Non-Nucleoside HIV-1 Reverse Transcriptase Inhibitors Studied by Targeted Molecular Dynamics Simulations

Fátima Rodríguez-Barrios,[†] Jan Balzarini,[‡] and Federico Gago*[,†]

Contribution from the Department of Pharmacology, University of Alcalá, E-28871 Alcalá de Henares, Madrid, Spain, and Rega Institute for Medical Research, K. U. Leuven, B-3000 Leuven, Belgium

Received December 22, 2004; E-mail: federico.gago@uah.es

Abstract: A series of targeted molecular dynamics simulations have been carried out in an attempt to assess the effect that the common Lys103Asn mutation in HIV-1 reverse transcriptase (RT) has on the binding of three representative non-nucleoside RT inhibitors (NNRTI), nevirapine, efavirenz, and etravirine. We have shown previously that, in the absence of an incoming inhibitor, creation of the NNRTI binding pocket is hampered due to the existence of a hydrogen bond between the side chains of Asn103 and Tyr188 for which no equivalent exists in the wild-type enzyme. As an extension of this work, we now apply the same methodology to drive the enzyme's conformation from the unbound state to the drug-bound state in the presence of the NNRTI. The location of each drug outside the binding pocket was determined by an automated docking program, and steering into the binding pocket followed a route that is likely to represent the actual entrance pathway. The additional hurdle to inhibitor entry imposed by the extra Asn103−Tyr188 hydrogen bond is seen to affect each NNRTI differently, with the ability to disrupt this interaction increasing in the order etravirine ≫ efavirenz ≥ nevirapine, in good accord with the experimental findings. This coherent picture strongly suggests that attempts to overcome resistance through structure-based drug design may be considerably more successful if dynamic structural aspects of the type studied here are considered, particularly in cases where binding energy-based structure−activity relationship methods are unable to provide the required information.

Introduction

The Lys103Asn (K103N) escape mutation in HIV-1 reverse transcriptase (RT) is selected very frequently both in vitro and in vivo by numerous non-nucleoside RT inhibitors (NNRTIs)[1] and is also commonly seen in patients receiving highly active antiretroviral therapy.[2,3] The location of Lys103 (or Asn103) at the outer rim of the pocket where NNRTIs bind implies that it is very seldom involved in direct interactions with the bound drugs.[4−6] This means that insight into the molecular basis of this particular resistance mutation is unlikely to be gained just from the static comparison of the complexes formed between the inhibitors and either the wild-type or the K103N mutant enzyme. For the same reason, the effect of this mutation is not amenable to structure−activity relationship studies that rely on differential interactions between a series of inhibitors and the whole[7] or parts of the protein[8] calculated for just one representative complex of each ligand. Nonetheless, important clues have been derived from several approaches including crystallographic and kinetic experiments and, more recently, theoretical calculations. Thus, early predictions of enhanced stabilization of the closed-pocket form of the K103N mutant RT in the unliganded state through hydrogen bonds that are not present in the wild-type enzyme[9] were later confirmed when the crystal structure of the K103N apoenzyme (PDB code 1HQE) was solved.[4] The proposed hydrogen bond between the side chains of Asn103 and Tyr188 was indeed observed and found to be additionally stabilized by interactions with two neighboring water molecules. Similar findings were reported for the complexes of the K103N mutant with HBY097 and loviride,[4] and also with efavirenz, PNU142721, and MSC194,[10] all of which consistently showed that the K103N substitution induced only minor positional

[†] University of Alcalá.
[‡] Rega Institute for Medical Research.

(1) Silvestri, R.; De Martino, G.; La Regina, G.; Artico, M.; Massa, S.; Vargiu, L.; Mura, M.; Loi, A. G.; Marceddu, T.; La Colla, P. *J. Med. Chem.* **2003**, *46*, 2482−2493.
(2) Schinazi, R. F.; Larder, B.; Mellors, J. W. *Int. Antivir. News* **2000**, *8*, 65−92.
(3) Stanford HIV sequence database 2002 (http://hivdb.Stanford.edu).
(4) Hsiou, Y.; Ding, J.; Das, K.; Clark, A. D., Jr.; Boyer, P. L.; Lewi, P.; Janssen, P. A. J.; Kleim, J. P.; Rösner, M.; Hughes, S. H.; Arnold, E. *J. Mol. Biol.* **2001**, *309*, 437−445.
(5) Gago, F.; et al. *J. Med. Chem.* **2001**, *44*, 1853−1865.
(6) Ren, J.; Milton, J.; Weaver, K. L.; Short, S. A.; Stuart, D. I.; Stammers, D. K. *Struct. Fold. Des.* **2000**, *8*, 1089−1094.
(7) Ajay; Murcko, M. A. *J. Med. Chem.* **1995**, *38*, 4953−4967.
(8) Rodríguez-Barrios, F.; Gago, F. *J. Am. Chem. Soc.* **2004**, *126*, 2718−2719.
(9) Esnouf, R.; Ren, J.; Ross, C.; Jones, Y.; Stammers, D.; Stuart, D. *Nat. Struct. Biol.* **1995**, *2*, 303−308.
(10) Lindberg, J.; Sigurosson, S.; Löwgren, S.; Andersson, H. O.; Sahlberg, C.; Noréen, R.; Fridborg, K.; Zhang, H.; Unge, T. *Eur. J. Biochem.* **2002**, *269*, 1670−1677.

10.1021/ja042289g CCC: $30.25

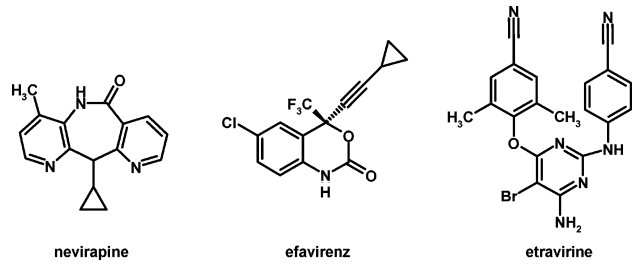

Figure 1. Chemical structures of the non-nucleoside RT inhibitors studied.

adjustments of the inhibitors and the residues lining the binding pocket relative to the respective complexes with wild-type RT. Additionally, determination of the association and dissociation rate constants (k_{on} and k_{off}, respectively) for nevirapine (Figure 1) binding to HIV-1 RT showed that the K103N mutation does not increase the k_{off} for this compound but instead decreases its k_{on} 5-fold.[11] This observation is in contrast with findings for other mutations that take place within the NNRTI binding pocket and also confer resistance to this drug (and many others). For example, Y181I and Y188L were shown to affect both k_{off} and k_{on} values, whereas L100I and V106A gave rise to 12- and 8.5-fold increases in the k_{off} values, respectively, without significantly influencing the k_{on}. Last, results of targeted molecular dynamics (tMD) simulations have recently supported the existence of a higher energy barrier for creation of the NNRTI binding pocket in the K103N mutant relative to the wild-type enzyme.[12]

Taken together, these three lines of evidence point to enhanced stabilization of the closed-pocket conformation that is predominant in the unbound state of HIV-1 RT as the primary resistance mechanism arising from the K103N mutation rather than a loss of interaction between the enzyme and the bound inhibitors (as seen for other mutants, e.g., Y181C and V106A). This would explain why so many structurally diverse classes of NNRTIs are affected by this amino acid substitution irrespective of their molecular scaffolds. Nonetheless, the fact that some promising second-generation NNRTIs,[13] for example, capravirine (formerly known as S-1153 and AG1549)[14] and etravirine (formerly known as TMC-125 and R165335),[15] display similar inhibitory efficacies against wild-type and the K103N RT mutant strongly suggests that these molecules are somehow able to overcome the extra energetic cost incurred on disrupting the hydrogen-bonding network reported above. Furthermore, the clinically used efavirenz also displays a slightly more favorable profile against viruses harboring the K103N mutation because resistance to this agent usually requires double mutations such as K103N+V108I and K103N+P225H.[16]

In an attempt to understand the improved inhibitory profile of some drugs (e.g., etravirine), but not others (e.g., nevirapine and efavirenz), in atomic detail while avoiding any subjective interpretation of available crystal structures, we have extended a previously reported tMD methodology.[12] This computational approach was useful earlier to confirm the existence of a higher energy barrier to binding-site creation in the K103N mutant relative to the wild-type enzyme, but those simulations were carried out in the absence of an incoming inhibitor. In the following, we describe how we have probed possible entrance pathways into the binding site of wild-type and the K103N mutant RT for nevirapine, efavirenz, and etravirine, as representatives of first- and second-generation NNRTIs for which at least one crystal structure has been determined in complex with one of these RT enzymes.

Materials and Methods

A. Experimental Methods. a. Compounds. Nevirapine was from Boehringer Ingelheim, ddGTP was from Sigma Chemical Ltd. (St. Louis, MO), and etravirine was from Tibotec-Virgo (Belgium). Efavirenz was kindly provided by Dr. R. Kirsh and Dr. J.-P. Kleim (at that time at Hoechst AG, Frankfurt, Germany).

b. Site-Directed Mutagenesis of HIV-1 RT. The mutant RT-enzyme containing the Lys103Asn mutation was derived from the RT sequence cloned in pKRT2His.[17] Site-directed mutagenesis was performed using the QuickChange Site-Directed Mutagenesis Kit (Stratagene, Westburg, Leusden, The Netherlands) as described before.[17b] The two synthetic oligonucleotide primers (Invitrogen Life Technologies, Merelbeke, Belgium) used contained the mutation at amino acid position 103 of HIV-1 RT. The presence of the K103N mutation was confirmed by sequencing of the RT gene on an ABI Prism 3100 sequencer (Applied Biosystems, Foster City, CA) using the ABI Prism Big Dye Terminator Cycle Sequencing Ready Reaction Kit (Applied Biosystems).

c. Expression of Mutant Recombinant HIV-1 RT. Recombinant HIV-1 RT was expressed from a two-plasmid coexpression system as previously described.[18] The p66 subunit of RT was expressed from pACYC66His and the p51 subunit from pKRT51. To construct wild-type and 103-mutated pACYC66His, wild-type and 103-mutated pKRT2His were digested with *Eco*RI and *Avi*II and the RT-containing fragments were ligated into pACYC184 digested with *Eco*RI and *Sca*I. To construct wild-type and 103-mutated pKRT51, wild-type and 103-mutated pKRT2His were digested with *Nco*I and *Kpn*I and the RT-containing fragment was ligated into pKRT51 digested with *Nco*I and *Kpn*I. Expression and purification of recombinant RT was performed as described previously.[17b]

d. Reverse Transcriptase Assay. For determination of the 50% inhibitory concentration (IC_{50}) of the test compounds against HIV-1 RT, the RNA-dependent DNA polymerase assay was performed as follows: the reaction mixture (50 μL) contained 50 mM Tris-HCl (pH 7.8), 5 mM DTT, 300 μM glutathione, 500 μM EDTA, 150 mM KCl, 5 mM $MgCl_2$, 1.25 μg of bovine serum albumin, a fixed concentration of the labeled substrate [^{3}H]dGTP (1.6 μM, 1 μCi; specific activity, 12.6 C_i/mmol; Amersham Pharmacia Biotech), a fixed concentration of the template/primer poly(rC)·oligo$(dG)_{12-18}$ (0.1 mM; Amersham Pharmacia Biotech), 0.06% Triton X-100, 5 μL of inhibitor solution [containing various concentrations (5-fold dilutions) of the compounds in the presence of a fixed concentration of 10% DMSO], and 5 μL of the RT preparations. The reaction mixtures were incubated at 37 °C for 30 min, at which time 200 μL of yeast RNA (2 mg/mL) and 1 mL of trichloroacetic acid (5%, v/v) in water were added. The solutions were kept on ice for at least 30 min, after which the acid-insoluble material was filtered over Whatman GF/C glass-fiber filters and washed 10 times with 2 mL of 5% trichloroacetic acid in water and one time with 70% ethanol. The filters were then analyzed for radioactivity in a liquid scintillation counter (Canberra Packard, Zellik, Belgium). The

(11) Maga, G.; Amacker, M.; Ruel, N.; Hubscher, U.; Spadari, S. *J. Mol. Biol.* **1997**, *274*, 738−747.
(12) Rodríguez-Barrios, F.; Gago, F. *J. Am. Chem. Soc.* **2004**, *126*, 15386−15387.
(13) Powels, R. *Curr. Opin. Pharmacol.* **2004**, *4*, 437−446.
(14) Fujiwara, T.; Sato, A.; el-Farrash, M.; Miki, S.; Abe, K.; Isaka, Y.; Kodama, M.; Wu, Y.; Chen, L. B.; Harada, H.; Sugimoto, H.; Hatanaka, M.; Hinuma, Y. *Antimicrob. Agents Chemother.* **1998**, *42*, 1340−1345.
(15) Arnold, E.; et al. *J. Med. Chem.* **2004**, *47*, 2550−2560.
(16) Erickson-Viitanen, S. K.; et al. *J. Med. Chem.* **2000**, *43*, 2019−2030.
(17) (a) D'Aquila, R. T.; Summers, W. C. *J. Acquired Immune Defic. Syndr.* **1989**, *2*, 579−587. (b) Pelemans, H.; Esnouf, R.; Jonckheere, H.; De Clercq, E.; Balzarini, J. *J. Biol. Chem.* **1998**, *273*, 34234−34239.
(18) Jonckheere, H.; Taymans, J. M.; Balzarini, J.; Velázquez, S.; Camarasa, M.-J.; Desmyter, J.; De Clercq, E.; Anné, J. *J. Biol. Chem.* **1994**, *269*, 25255−25258.

IC_{50} for each test compound was determined as the compound concentration that inhibited HIV-1 RT activity by 50%.

B. Computational Methods. a. Quantum Mechanics Calculations. The geometries of nevirapine, etravirine, and efavirenz were optimized using the ab initio quantum chemistry program Gaussian 98[19] and the HF/3-21G* basis set. A set of atom-centered RHF 6-31G*//3-21G* charges for each inhibitor was then obtained by using the RESP methodology,[20] as implemented in the AMBER suite of programs (http://amber.scripps.edu/). Covalent and nonbonded parameters for the inhibitor atoms were assigned, by analogy or through interpolation, from those already present in the AMBER force field[21] (parm99), or consistently derived, as explained in more detail elsewhere.[5,22,23]

b. Molecular Docking. Different conformers of nevirapine, etravirine, and efavirenz, generated by randomly changing torsion angles, were docked in different orientations near the putative entrance to the NNRTI binding site in HIV-1 RT using the genetic algorithm implemented in AutoDock[24] and the wild-type unliganded (apoenzyme) form of RT (PDB code 1DLO)[25] as the target protein. A volume for exploration was defined in the shape of a three-dimensional cubic grid ($27 \times 27 \times 28$ Å^3) with a spacing of 0.3 Å that enclosed the residues that are known to make up the NNRTI binding pocket in the p66 subunit and a long portion of the intersubunit cleft, including the surroundings of Glu138 in the p51 subunit. At each grid point, the receptor's atomic affinity potentials for carbon, oxygen, nitrogen, sulfur, chlorine, fluorine, bromine, and hydrogen atoms were precalculated for rapid intra- and intermolecular energy evaluation of the docking solutions for each inhibitor. Despite the relatively wide variety of binding modes found by the automated docking program in the region delimited for exploration, most of the solutions were placed at the mouth of the putative entrance to the NNRTI binding pocket-to-be.

To obtain additional validation of the proposed binding mode for the more flexible etravirine, program GRID (http://www.moldiscovery.com/)[26] was also used to search for sites on the enzyme that could be complementary to the functional groups present in this inhibitor. For the GRID calculations, a 25 Å × 25 Å × 25 Å lattice of points spaced at 0.5 Å was established at the putative entrance close to the interface between the β7-β8 loop in p51 and the p66 subunit. The probes used were C1= (aromatic carbon), N:# (sp nitrogen with lone pair), and BR (bromine). The dielectric constants chosen were 4.0 for the macromolecule and 80.0 for the bulk water.

c. Molecular Dynamics Simulations. The macromolecular assemblies composed of the unliganded forms of heterodimeric wild-type (PDB code 1DLO)[25] or K103N mutant (PBD code 1HQE)[4] HIV-1 RT and each inhibitor predocked at the entrance of the binding cavity were solvated with a 20 Å-radius shell of TIP3P water molecules centered on Tyr188 of the p66 subunit. Each assembly was gradually refined in AMBER using a cutoff of 11.0 Å and a distance-dependent dielectric constant ($\epsilon = r_{ij}$) for dampening the electrostatic interactions. Given that the NNRTI binding site is close to the surface of the protein, and that only a "cap" of water molecules was used due to the large computational burden, a macroscopic dielectric constant is warranted as the full dampening effect of the solvent is not present.[27] First, only the water molecules were allowed to reorient, and then the water molecules and all protein side chains were allowed to relax. In each case, 500 steps of steepest descent were followed by conjugate gradient energy minimization until the root-mean-square (rms) value of the potential energy gradient was <0.01 kcal mol^{-1} Å^{-1}. The refined structures were then heated and equilibrated at 300 K for 100 ps prior to the tMD simulations at the same temperature during which the trajectories were biased so as to force pocket formation in the presence of the incoming inhibitor.

The structures used as end-points in the tMD simulations were: for nevirapine, the experimental complexes with either wild-type HIV-1 RT (PDB code 1VRT)[28] or the K103N mutant enzyme (PDB code 1FKP);[6] for efavirenz, the experimental complexes with wild-type and K103N HIV-1 RT (PDB codes 1IKW and 1IKV, respectively);[10] and for etravirine, the X-ray complex with K103N RT (PDB code 1SV5)[15] and, in the absence of an experimental structure, the same complex with Asn103 replaced with Lys. All of these target structures were solvated and adapted to the AMBER force field as reported above for the initial structures.

The tMD approach[29,30] was essentially as described[12] and made use of the standard implementation recently incorporated into AMBER (version 8.0),[31] which allows the solvent molecules to move freely and follow the dynamics of the protein. A restraint was defined in terms of a mass-weighted rms superposition to the final reference structure (target) and applied in the force field as an extra energy term of the following form:

$$E = 0.5k_rN(\text{rmsd} - \text{trmsd})^2$$

where k_r is the force constant, N is the number of atoms, and trmsd is the target rms deviation, which we set to zero. A force constant of 0.5 kcal mol^{-1} Å^{-2} over 0.5 ns proved sufficient to find a low-energy path leading from the simulated structure to the target structure using only the heavy atoms of both protein and ligand in the rms definition. Note that this implementation is slightly different from that used previously for the enzyme alone in which the force constant was applied to all atoms.[12]

Results and Discussion

General Considerations. In the process of cavity creation that accompanies NNRTI binding to the allosteric site in HIV-1 RT, the side chains of Tyr188 and Tyr181 reorient by "flipping" toward the polymerase active site. In the presence of the K103N mutation, however, formation of a good hydrogen bond between the phenol oxygen of Tyr188 and the side-chain carboxamide of Asn103 was early suggested to hamper this rotation, thereby increasing the stabilization of the closed-pocket form of this mutant enzyme.[9] Crystallographic evidence[4,10] and results from tMD simulations[12] have provided support to this hypothesis, which is in agreement with kinetic data,[11] but to the best of our knowledge a comparative assessment of the binding of resilient and nonresilient NNRTIs to both the K103N mutant and the wild-type enzymes has not been reported.

In Vitro Activity of Several Representative HIV-1 Inhibitors. Etravirine (Figure 1) is an example of a second-generation NNRTI with a potency against wild-type HIV-1 RT and a wide range of HIV-1 RT mutants that appears to arise from its ability

(19) Pople, J. A.; et al. *Gaussian 98*, revision A.11.2; Gaussian, Inc.: Pittsburgh, PA, 2001.
(20) Bayly, C. I.; Cieplak, P.; Cornell, W. D.; Kollman, P. A. *J. Phys. Chem.* **1993**, *97*, 10269−10280.
(21) Cornell, W. D.; Cieplak, P.; Bayly, C. I.; Gould, I. R.; Merz, K. M.; Ferguson, D. M.; Spellmeyer, D. C.; Fox, T.; Caldwell, J. W.; Kollman, P. A. *J. Am. Chem. Soc.* **1995**, *117*, 5179−5197.
(22) Kmunicek, J.; Luengo, S.; Gago, F.; Ortiz, A. R.; Wade, R. C.; Damborsky, J. *Biochemistry* **2001**, *40*, 8905−8917.
(23) de la Fuente, J. A.; Manzanaro, S.; G. de Quesada, T.; Reymundo, I.; Luengo, S. M.; Gago, F. *J. Med. Chem.* **2003**, *46*, 5208−5221.
(24) AutoDock: Automated docking of flexible ligands to receptors, Version 3.0, 1999; Morris, G. M.; Goodsell, D. S.; Huey, R.; Hart, W. E.; Halliday, S.; Belew, R.; Olson, A. J. The Scripps Research Institute, La Jolla, CA 92037-1000.
(25) Hsiou, Y.; Ding, J.; Das, K.; Clark, A. D., Jr.; Hughes, S. H.; Arnold, E. *Structure* **1996**, *4*, 853−860.
(26) Goodford, P. *J. Med. Chem.* **1985**, *28*, 849−857.
(27) Ortiz, A. R.; Pisabarro, M. T.; Gago, F. *J. Med. Chem.* **1993**, *36*, 1866−1879.
(28) Stammers, D.; et al. *Nat. Struct. Biol.* **1995**, *2*, 293−302.
(29) Ma, J.; Karplus, M. *Proc. Natl. Acad. Sci. U.S.A.* **1997**, *94*, 11905−11910.
(30) Ma, J. P.; Sigler, P. B.; Xu, Z. H.; Karplus, M. *J. Mol. Biol.* **2000**, *302*, 303−313.
(31) http://amber.scripps.edu/doc8/amber8.pdf.

Table 1. Inhibitory Activity against Wild-type and Lys103Asn HIV-1 Reverse Transcriptases of Several Representative RT Inhibitors Belonging to Different Classes

	IC_{50} (μM)[a]	
	wild-type	K103N
nevirapine	0.39 ± 0.085	>10
efavirenz	0.004 ± 0.002	0.14 ± 0.064
etravirine	0.029 ± 0.014	0.032 ± 0.015
capravirine	0.005 ± 0.001	0.004 ± 0.001
TSAO-m^{3}T	0.85 ± 0.085	8.5 ± 0.57
ddGTP	0.037 ± 0.002	0.016 ± 0.003
PFA (foscarnet)	5.4 ± 0.49	2.5 ± 0.74

[a] 50% inhibitory concentration or compound concentration required to inhibit recombinant HIV-1 RT by 50%. Template/primer: (poly)rC·(oligo)dG; radiolabeled substrate: [^{3}H]dGTP.

to adopt multiple conformations and orientations in the binding pocket.[15] When we determined the concentration of this compound required to inhibit recombinant HIV-1 RT by 50% (IC_{50}), virtually no differences were found between wild-type and K103N mutant enzymes (Table 1), in agreement with data reported by other authors.[13] This was also the case for phosphonoformic acid (PFA, foscarnet) and 2′,3′-dideoxyguanosine-5′-triphosphate (ddGTP), which act through different mechanisms at the RT active site,[32] and for capravirine,[14] another second-generation NNRTI that is known to establish, at least with wild-type RT, an extensive network of hydrogen bonds involving main chain atoms of residues 101, 103, and 236 in the p66 subunit.[33] On the contrary, the same mutation was found to increase the IC_{50} of nevirapine and efavirenz by more than 20- and 35-fold, respectively, again in good accord with comparable data from the literature.[10]

Placement of the NNRTIs Studied at the Putative Entrance to the NNRTI Binding Site. The NNRTI binding pocket is located close to, but distant from, the substrate binding site and consists primarily of Leu100, Lys101, Lys103, Val106, Thr107, Val108, Val179, Tyr181, Tyr188, Val189, Gly190, Phe227, Trp229, Leu234, and Tyr318 in the p66 subunit.[34] The putative entrance to this pocket is proposed to be located at the interface of the p66/p51 heterodimer and is principally formed by Pro95, Leu100, Lys101, Lys103, Val179, and Tyr181 of p66,[28,34] together with Glu138 from the p51 subunit. This is the same entrance that was considered in the study of the "unbinding" process of α-anilinophenyl-acetamide (α-APA) from RT using a steered MD simulation in which a harmonic potential was applied to the inhibitor to pull it out from the binding pocket.[35] Other authors, however, based on the X-ray crystal structure of the bis(heteroaryl) piperazine (BHAP), U-90152, and the fact that the Glu138→Lys mutation does not result in marked losses of sensitivity to most NNRTIs[36] (with the exception of the rather unique TSAO derivatives),[37] have proposed an alternative entry pathway through a channel originating in Pro236.[38]

Two of the most populated clusters found by AutoDock for nevirapine were placed at the entrance to the binding pocket. The largest one provided a reasonable entry point and consisted of molecules having their carbonyl oxygen located in the same position that is occupied by a water molecule in the unliganded crystal structures of both wild-type and Lys103Asn mutant HIV-1 RT.[4] This water molecule forms only a weak hydrogen bond with the peptide nitrogen of Lys101 in the unliganded wild-type HIV-1 RT structure, whereas in the Lys103Asn mutant it forms a second hydrogen bond with the side chain phenol group (Oη) of Tyr181. The nevirapine molecule with the highest score in this cluster was selected as representative of the predocked complex (Figure 2). As a consequence, in the location that was found, the amide nitrogen (N11) of nevirapine forms a hydrogen bond with the hydroxyl group of Tyr181. Besides, the cyclopropyl group points toward the solvent, the "methylated wing" is situated over the side chains of Ile135 and Asn136 in the p51 subunit, and the other "wing" is accommodated near a hydrophobic patch made up of the side chains of Leu100, Lys101, and Val179 in the p66 subunit.

For efavirenz, two clusters were found to be considerably more populated than the rest, but only one was situated at the mouth of the NNRTI binding pocket. The conformer that we chose from this latter cluster was the one with the highest score, which shows the O10 of the benzoaxine-2-one ring of the drug forming a hydrogen bond with the NH of Ile135 in the p51 subunit, the cyclopropylethynyl group placed over the side chain of this same residue in such a way that it points toward the entry to the cavity, and the trifluorophenyl group situated in front of the peptide amide group of Glu138 and Thr139 also in the smaller subunit (Figure 3).

Because the high flexibility of etravirine largely prevented any clustering, program GRID[26] assisted in the selection of the preferred docking site. Thus, the solution chosen was that in which the functional groups of the molecules best matched the calculated interaction energy maps: the pyrimidine amino group appeared hydrogen bonded to both the carboxylate group of Glu138 and the carbonyl group of Ile135 in the p51 subunit, and the 1,4-cyanophenyl moiety (ring II) was accommodated into a hydrophobic pocket lined by the hydrocarbon side chains of Leu100, Lys101, and Val179 of p66 (Figure 4).

Overall, this docking procedure provided us with a location for each drug that was taken as an unbiased and reasonable entry point for starting the subsequent tMD procedure. Remarkably, this location at the interface between the two subunits was reminiscent of the binding site proposed[5] for the unique class of TSAO compounds,[37] which are known to interfere with enzyme dimerization.[39]

Targeted Molecular Dynamics Simulations. The closed-pocket forms of the whole wild-type and K103N RT heterodimers (987 residues in all), as found in PDB entries 1DLO[25] and 1HQE,[4] but with the NNRTI bound at the putative entrance to the pocket as explained above, were gradually forced to adopt the conformation of their NNRTI-docked counterparts during an MD trajectory lasting 0.5 ns. In the initial apo-like conformation, the enzyme's p66 thumb subdomain is folded down into the DNA binding cleft where it makes contacts with the tip of

(32) De Clercq, E. *J. Clin. Virol*. **2004**, *30*, 115−133.
(33) Ren, J.; Nichols, C.; Bird, L. E.; Fujiwara, T.; Sugimoto, H.; Stuart, D. I.; Stammers, D. K. *J. Biol. Chem*. **2000**, *275*, 14316−14320.
(34) Arnold, E.; et al. *Structure* **1995**, *3*, 365−379.
(35) Shen, L.; Shen, J.; Luo, X.; Cheng, F.; Xu, Y.; Chen, K.; Arnold, E.; Ding, J.; Jiang, H. *Biophys. J*. **2003**, *84*, 3547−3563.
(36) Balzarini, J.; Kleim, J. P.; Riess, G.; Camarasa, M. J.; De Clercq, E.; Karlsson, A. *Biochem. Biophys. Res. Commun*. **1994**, *201*, 1305−1312.
(37) Camarasa, M. J.; San-Félix, A.; Velásquez, S.; Pérez-Pérez, M. J.; Gago, F.; Balzarini, J. *Curr. Top. Med. Chem.* **2004**, *4*, 945−963.
(38) Esnouf, R. M.; Ren, J.; Hopkins, A. L.; Ross, C. K.; Jones, E. Y.; Stammers, D. K.; Stuart, D. I. *Proc. Natl. Acad. Sci. U.S.A*. **1997**, *94*, 3984−3989.
(39) Sluis-Cremer, N.; Dmitrienko, G. I.; Balzarini, J.; Camarasa, M. J.; Parniak, M. A. *Biochemistry* **2000**, *39*, 1427−1433.

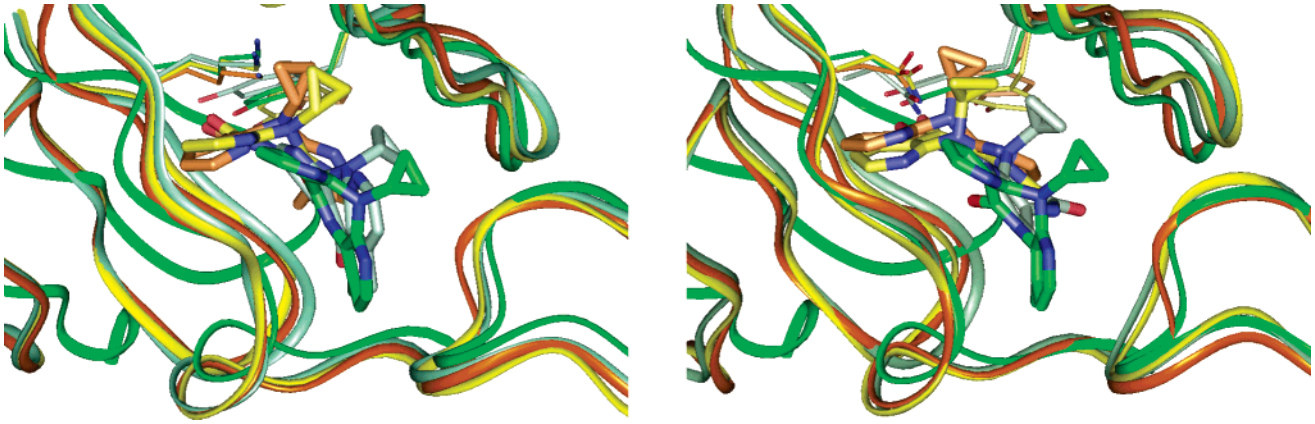

Figure 2. Overlay of representative snapshots from the tMD trajectory showing the evolution of the position of nevirapine and relevant RT residues as the NNRTI migrates from the predocked site at the putative entrance into the NNRTI binding pocket. The RT Cα trace is represented as a ribbon, and, for clarity, only the side chains of Tyr188 and either Lys103 (left) or Asn103 (right) are shown as thin sticks. The β7-β8 loop of the p51 subunit is displayed on the bottom right of each figure. Ribbon and inhibitor carbon atoms have been colored according to time frames so that time evolution goes in the order green→gray→yellow→orange (wild-type, 0, 360, 415, and 500 ps; K103N, 0, 330, 340, and 500 ps).

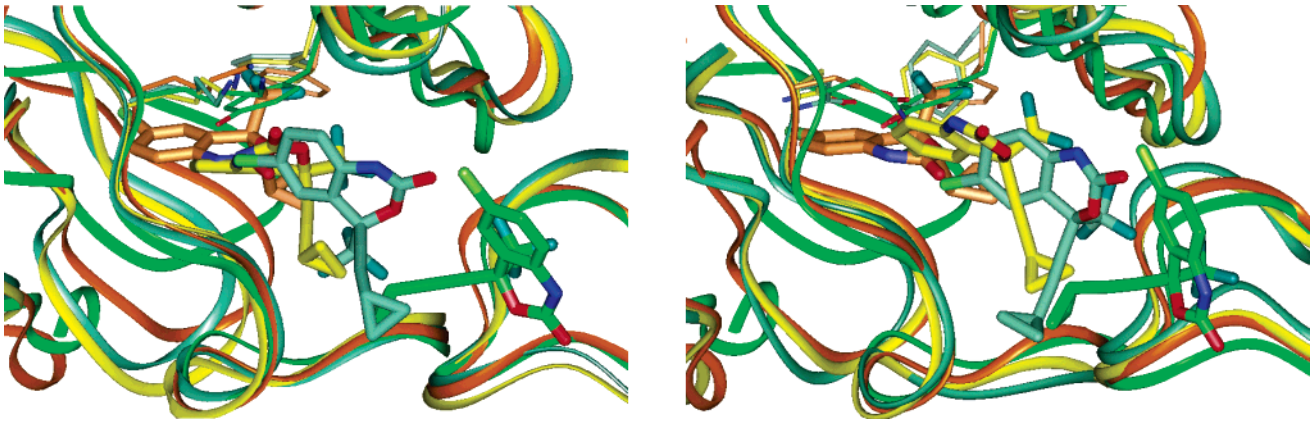

Figure 3. Overlay of representative snapshots (wild-type, 0, 320, 360, and 500 ps; K103N, 0, 315, 322, and 500 ps) from the tMD trajectory showing the evolution of the position of efavirenz and relevant RT residues as the NNRTI migrates from the predocked site at the putative entrance into the NNRTI binding pocket. Color schemes, orientation, and display are as explained in the legend to Figure 2.

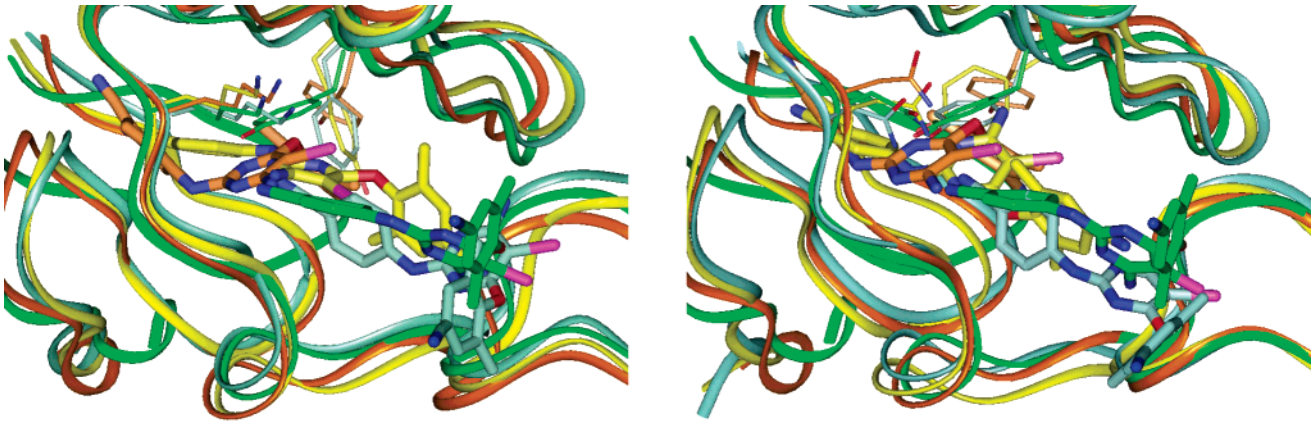

Figure 4. Overlay of representative snapshots (wild-type, 0, 250, 290, and 500 ps; K103N, 0, 250, 290, and 500 ps) from the tMD trajectory showing the evolution of the position of etravirine (bromine atom in magenta) and relevant RT residues as the NNRTI migrates from the predocked site at the putative entrance into the NNRTI binding pocket. Color schemes, orientation, and display are as explained in the legend to Figure 2.

the fingers.[40] Nonetheless, we must note that the structure of an unliganded HIV-1 RT that was produced by soaking out the weakly binding NNRTI, 1-[(2-hydroxyethoxy)methyl]-6-(phenylthio)thymine (HEPT), from pregrown crystals revealed only minor rearrangements in this subdomain.[9] At any rate, as the simulation progresses, the p66 thumb subdomain opens up and gradually extends away from the p66 fingers toward the target bound conformation (Supporting Information, Figure S1).[41]

(40) Rodgers, D. W.; Gamblin, S. J.; Harris, B. A.; Ray, S.; Culp, J. S.; Hellmig, B.; Woolf, D. J.; Debouck, C.; Harrison, S. C. *Proc. Natl. Acad. Sci. U.S.A.* **1995**, *92*, 1222−1226.

(41) (a) Arnold, E.; et al. *Proc. Natl. Acad. Sci. U.S.A.* **1993**, *90*, 6320−6324. (b) Huang, H.; Chopra, R.; Verdine, G. L.; Harrison, S. C. *Science* **1998**, *282*, 1669−1675.

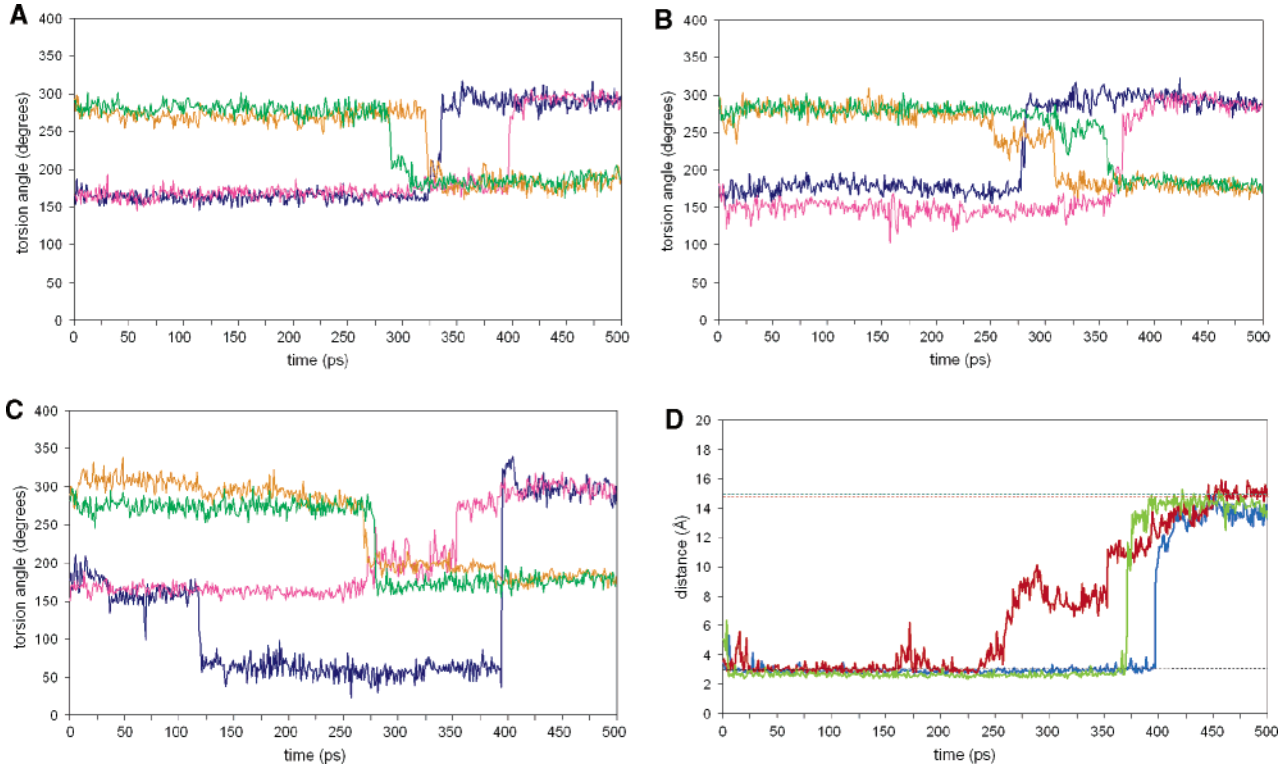

Figure 5. Time evolution along the tMD simulations of the N−CA−CB−CG dihedral angles of Y188 (blue, wt; magenta, K103N mutant) and Y181 (orange, wt; green, K103N mutant) side chains in the complexes of HIV-1 RT with (A) nevirapine, (B) efavirenz, and (C) etravirine. (D) Time evolution of the distance between side chain atoms Oη of Tyr188 and either Nδ2 (blue, nevirapine; red, etravirine) or Oδ2 (green, efavirenz) of Asn103. The broken lines represent the same distances as found in the X-ray crystal structures of unliganded (bottom) and NNRTI-bound (top) K103N RT.

Concomitant with this, the β12-β13-β14 sheet (the "primer grip") is displaced so that the β12-β13 hairpin containing Phe227 and Trp229 (the back wall and floor, respectively, of the hydrophobic pocket where the inhibitors will eventually bind)[28,34,40] is repositioned so that it now allows rotation of the side chains of Tyr181 and Tyr188 (Figure 5A−C). This is accompanied by the reported improper geometry of the catalytic aspartic acid residues 110, 185, and 186 at the polymerase active site that may result in enzyme inhibition,[9,42] together with other proposed mechanisms such as hampering of some critical motions that are essential for the enzyme to perform catalysis and/or mispositioning of the nucleic acid template/primer substrate and the incoming dNTP.[43,44]

The process of pocket creation in the presence of the NNRTI was similar to that studied in its absence,[12] with one notable exception: when the side-chain conformations of Tyr181 and Tyr188 were monitored by measuring the evolution of their N−CA−CB−CG dihedral angles, reorientation of Tyr188 was previously found to systematically precede that of Tyr181, whereas no such clear trend is observed in the present simulations (Figure 5). Because the inhibitors are now pushing their way into the binding pocket, the number and magnitude of the local barriers that have to be overcome to create the cavity and let the inhibitor in must be slightly different. In fact, the nature of these barriers appears to depend on the plasticity of the NNRTI as three different Y188 rotamers are observed in the simulation of etravirine with wild-type RT, whereas only two are detected in the simulations with the less flexible nevirapine and efavirenz. In any case, flipping of Tyr188 to adopt the pocket conformation in the K103N RT mutant enzyme is seen, in both sets of simulations,[12] to be closely coupled to the breaking of the hydrogen bond between Asn103 and Tyr188 (Figure 5D). It is also apparent that this hydrogen bond is more easily broken when the NNRTI opening its way into the pocket-to-be is etravirine, in consonance with the resilience of this inhibitor to the effect of the K103N mutation (Table 1).

The progression of the conformational changes in the enzyme leading to creation of the NNRTI binding pocket, as well as the process of inhibitor entry into the cavity, were monitored by measuring the evolution of the rms deviation (rmsd) of both protein backbone atoms and inhibitor atoms along the simulation time (Figure 6). It can be clearly seen that, whereas the rmsd values decrease equally gradually and are virtually superimposable for the backbones of both proteins, the corresponding values for the inhibitors fall rather sharply and significant differences are apparent when the complexes of nevirapine and efavirenz with either the wild-type or the mutant enzyme are compared. The rmsd plateaus that are observed in the simulations of K103N HIV-1 RT with these two NNRTIs during the 300−400 ps period (Figure 6A,B) reflect the greater difficulty (longer times) in achieving the bound conformation in this mutant enzyme relative to wild-type. This delay is coincident with the longer time (and therefore higher energy) that is required to disrupt the hydrogen bond between Asn103 and Tyr188 in these two complexes when compared to the etravirine complex (Figure 5D). In contrast, the smooth drops in rmsd for etravirine in both complexes nicely overlap (Figure 6C), reflecting that the breaking of this hydrogen bond does not

(42) Ren, J.; Stammers, D. K. *Trends Pharmacol. Sci.* **2005**, *26*, 4−7.
(43) Sarafianos, S. G.; Das, K.; Hughes, S. H.; Arnold, E. *Curr. Opin. Struct. Biol.* **2004**, *14*, 716−730.
(44) Sluis-Cremer, N.; Temiz, N. A.; Bahar, I. *Curr. HIV Res.* **2004**, *2*, 323−332.

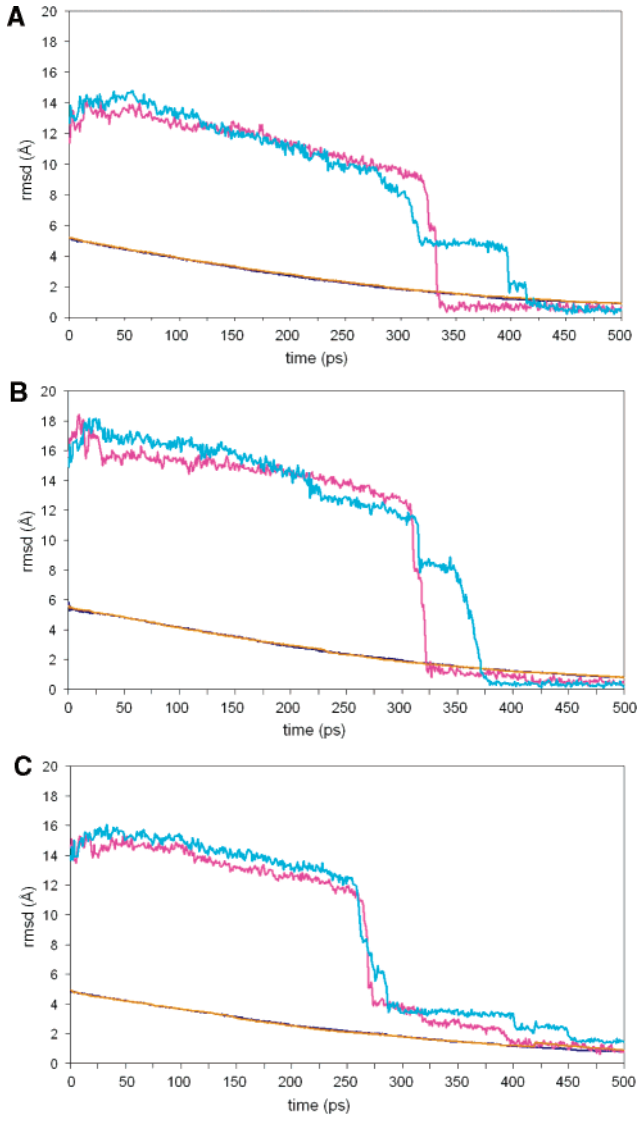

Figure 6. Time evolution of the mass-weighted root-mean-square deviation (rmsd) of wild-type and K103N HIV-1 RT backbone (blue and orange, respectively) and inhibitor atoms (magenta and cyan, respectively) along the simulation time for (A) nevirapine, (B) efavirenz, and (C) etravirine.

hamper entry of this inhibitor into the binding pocket. This can be taken to mean that cavity creation takes place when equivalent amounts of energy have been pumped into both systems. On the contrary, in the case of nevirapine and efavirenz, the need to overcome the additional hurdle imposed by the presence of this extra hydrogen bond makes pocket creation and NNRTI binding more difficult, and this accounts for the substantial increase in drug concentration that is required to effect the same degree of enzyme inhibition (Table 1).

Because our results strongly suggested that the cyano substituent on ring II of etravirine could compete with the Asn103-Tyr188 hydrogen bond in the predocked complex that this drug is proposed to form with the K103N mutant RT (Figures 4 and 7A), the distances between the side-chain atom Nδ2 of Asn103 and both the Oη of Tyr188 and the cyano nitrogen of etravirine were monitored (Figure 7B). It can be seen that both hydrogen-bonding distances are comparable at the beginning of the simulation but only that involving the protein residues is maintained from 25 to 150 ps. Later, the drug outcompetes Tyr188 until, finally, both hydrogen bonds are lost in the docked complex corresponding to the X-ray crystal structure.[15]

The feasibility of such NNRTI-RT interaction was assessed by searching for similar ones in other ligand−protein complexes present in the Protein Data Bank using the ReLiBase[45] data retrieval system (http://relibase.ebi.ac.uk/). Several examples were indeed found, the most similar one being that taking place between the amide side chain of Asn768 in xanthine dehydrogenase and the cyano group present in inhibitor TEI-6720 (PDB accession code 1N5X). Interestingly, another NNRTI described in the literature, the phenylethylthiazolylthiourea (PETT) analogue MSC194, which also has a cyano substituent in a similar position, has nanomolar potency against wild-type RT that is reduced only 10-fold against the K103N mutant.[10]

Final Considerations. The change at position 103 of HIV-1 RT from lysine (codons AAA and AAG) to asparagine (codons AAU and AAC) was rather intriguing for some time: despite being the most commonly observed NNRTI resistance mutation in the clinic, giving wide cross-resistance to most NNRTIs,[46] this residue was only seldom seen to be involved in direct interactions with the inhibitors. The proposal that the resistance evoked by this mutation could be due to stabilization of the unliganded conformation of the enzyme by the formation of a hydrogen bond between the asparagine side chain and the hydroxyl group of Tyr188[9] found experimental support when the crystal structure of the K103N RT enzyme was solved.[4] Later, it was shown that creation of the cavity using a tMD approach required the use of higher force constants (or longer simulation times) to overcome the local energy barrier in the case of the K103N mutant RT than in the case of the wild-type enzyme.[12]

At least in theory, the effect of stabilization of the unliganded form of the enzyme could be counterbalanced if a hydrogen bond could be formed between the asparagine side chain and a suitable moiety present at the right position in the incoming inhibitor. Despite the fact that up to now this has been mostly a trial-and-error exercise, principally achieved by focusing on the ligand already docked within the NNRTI binding pocket, some examples of success have already been published. A very significant one is capravirine,[14] which shows no loss of potency for the Lys103→Asn mutation (Table 1), even though in the presence of this drug a threonine (encoded as ACA/ACC/ACG/ACU) rather than an asparagine is selected as an escape mutation at position 103 in place of lysine. Based on the present results, and in the absence of a cocrystal structure with the mutant enzyme, we can speculate that resilience of capravirine to the Lys103→Asn mutation could be due to the carbamate group being able to disrupt the hydrogen bond between Lys103 and Tyr188 in a way similar to that reported here for the cyano group of etravirine. Nonetheless, because this inhibitor establishes an extensive network of hydrogen bonds with main chain protein atoms,[33] side-chain changes affect its inhibitory potency much less than is the case for other NNRTIs. In fact, tissue culture experiments have shown that for HIV-1 to escape capravirine, multiple mutations in RT are required, for example, Val106→Ala and Phe227→Leu or Lys103→Thr, Val106→Ala, and Leu234→Ile.[14]

(45) Hendlich, M.; Bergner, A.; Günther, J.; Klebe, G. *J. Mol. Biol.* **2003**, *326*, 607−620.
(46) Schinazi, R. F.; Larder, B. A.; Mellors, J. W. *Int. Antivir. News* **1997**, *5*, 129−135.

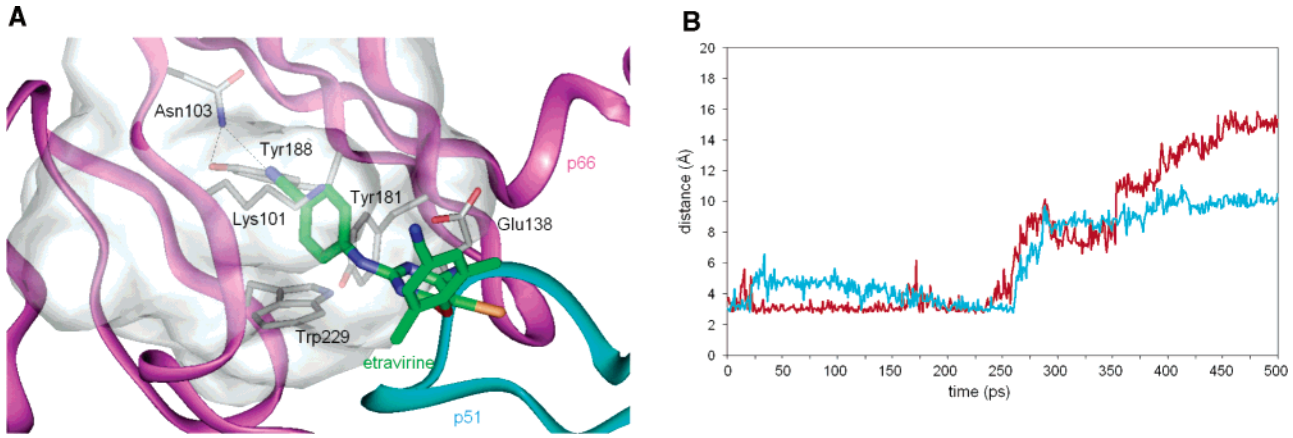

Figure 7. (A) Proposed docking site for etravirine at the entrance to the NNRTI binding pocket of K103N HIV-1 RT. The Cα trace of the enzyme is displayed as a ribbon, colored in pink and cyan for the p66 and p51 subunits, respectively. The side chains of (counterclockwise from the top) Asn103, Tyr188, Lys101, Trp229, Tyr181, and p51-Glu138 are shown as thin sticks, with carbon atoms colored in gray. Etravirine is displayed as thick sticks, with carbon atoms colored in green and the bromine atom colored in orange. The residues making up the NNRTI binding pocket are enveloped by a semitransparent solvent-accessible surface. (B) Time evolution of the distances (shown as dotted lines in A) between side-chain atoms Nδ2 of Asn103 and Oη of Tyr188 (red) and between Nδ2 of Asn103 and the cyano substituent on ring II of etravirine (cyan).

In this regard, it is of interest to analyze, in light of the results presented here, why resistance to efavirenz usually requires an additional mutation such as V108I or P225H besides that of K103N. Given the close proximity of the side chain of Val108 to the phenol ring of Tyr188, our simulations suggest that rotation of this ring during the process of pocket formation would be further hampered in the presence of the additional methyl group of an isoleucine at this position. This hypothesis needs further exploration but may provide a satisfactory explanation to the observation that resistance is evoked despite the fact that most NNRTIs, including efavirenz, do not contact this residue in wild-type RT. In support of this claim is the observation that the greatest change observed in V108I RT is found at the distally positioned Tyr181, which is >8 Å from the mutation site.[47] In the case of Pro225, which precedes the β12 strand (226−230), a mutation to His could affect the reported motions involving the β12-β13 hairpin, thereby also hampering pocket creation.

Insight into the flexibility of the different domains present in HIV-1 RT has been gained from visual comparison of many different crystal structures and also from application of a variety of computational methods including both the Gaussian network model of proteins[48] and standard[35,49] as well as steered[35] MD simulations. The present methodology represents a novel computational shortcut to study the binding of inhibitors to HIV-1 RT and can possibly be extended to other NNRTIs with the ability to bind in more than one conformation, such as the diaryltriazine (DATA) and diarylpyrimidine (DAPY) derivatives that led to rilpivirine,[50] as well as to others that require the motion of only Tyr188 (e.g., HEPT)[51] or neither Tyr181 nor Tyr188 (e.g., CP-94,707).[52] In light of the useful information obtained herein for etravirine, and the clear distinctions established with respect to nevirapine and efavirenz, the hints provided by this type of simulations are likely to be of value in the design of novel resistance-evading inhibitors. Nevertheless, we are aware that more simulations, longer simulation times, and extensions to other inhibitors and mutant enzymes will be necessary to further validate this approach and expand our understanding of how to overcome this therapeutically important problem.

Conclusions

Lys103Asn is a clinically relevant mutation that hampers the binding of and confers resistance to many classes of structurally diverse NNRTIs inhibitors including efavirenz. Although it could be thought in principle that, in common with other frequent mutant RT enzymes, individual differences in efficacy between related NNRTIs could arise from differential interactions between the inhibitors and specific protein residues,[8] crystallographic studies with the K103N mutant enzyme have revealed a notable absence of specific interactions involving the N103 side chain.[6,10,15] On the other hand, evidence for enhanced stabilization of the closed-pocket form of the K103N mutant RT through Asn103−Tyr188 side-chain hydrogen bonding was obtained when the crystal structure of the K103N apoenzyme was solved.[4] Support for this view was later gained when tMD simulations showed the existence of a higher energy barrier to pocket creation in this mutant enzyme relative to wild-type.[12] The present results, in the presence of an incoming inhibitor, confirm previous findings, hint at plausible ways for NNRTI entry into the pocket, and further suggest that resilience to the insidious effects of the irksome K103N mutation can be attained by designing ligands that are able to disrupt the Asn103−Tyr188 interaction as they gain access into the binding site pocket rather than when they are already docked within the pocket, hence the necessity of studying these systems in a dynamic context. Furthermore, the intermediary protein structures that can be extracted from the tMD trajectories can provide alternative targets for ligand docking studies.

The development of etravirine[15] and rilpivirine[50] exemplifies the successful application, by a multidisciplinary team, of the concept of exploiting conformational degrees of freedom to offset the effects of resistance mutations. Implementation of the

(47) Ren, J.; Nichols, C. E.; Chamberlain, P. P.; Weaver, K. L.; Short, S. A.; Stammers, D. K. *J. Mol. Biol.* **2004**, *336*, 569−578.
(48) (a) Bahar, I.; Erman, B.; Jernigan, R. L.; Atilgan, A. R.; Covell, D. *J. Mol. Biol.* **1999**, *285*, 1023−1037. (b) Temiz, N. A.; Bahar, I. *Proteins* **2002**, *49*, 61−70.
(49) (a) Madrid, M.; Jacobo-Molina, A.; Ding, J.; Arnold, E. *Proteins* **1999**, *35*, 332−337. (b) Madrid, M.; Lukin, J. A.; Madura, J. D.; Ding, J.; Arnold, E. *Proteins* **2001**, *45*, 176−182.
(50) Janssen, P. A. J.; et al. *J. Med. Chem.* **2005**, *48*, 1901−1909.
(51) Stuart, D. I.; et al. *J. Med. Chem.* **1996**, *39*, 1589−1600.
(52) Pata, J. D.; Stirtan, W. G.; Goldstein, S. W.; Steitz, T. A. *Proc. Natl. Acad. Sci. U.S.A.* **2004**, *101*, 10548−10553.

methodology we now describe during the design process might help to devise alternative or complementary strategies to modify other lead compounds in such a way that they can circumvent the ability of RT enzymes harboring the common K103N substitution (and possibly other mutations) to escape the potency of the inhibitors. The method also opens new possibilities in the study of alternative entry pathways into the NNRTI binding pocket, as proposed, for example, for BHAP derivatives[38] and CP-94,707.[52]

Acknowledgment. This paper is dedicated to Professor José Elguero (IQM, CSIC, Madrid) on the occasion of his 70th birthday. We thank Kristien Minner for excellent technical assistance. Financial support from the European Commission (no. QLRT-2000-30291 and HPAW-2002-10004), the "Fonds voor Wetenschappelijk Onderzoek − Vlaanderen" (no. G-0267-04 to J.B.), the Spanish CICYT (SAF2003-7219-C02 to F.G.), and the National Foundation for Cancer Research (to F.G.) are gratefully acknowledged. F.R.-B. is a fellow of the Spanish Ministerio de Ciencia y Tecnología.

Supporting Information Available: Complete refs 5, 15, 16, 19, 28, 34, 41a, 50, and 51, one additional figure showing the separate evolutions of the rmsd of the thumb domain and the β12-β13-β14 sheet along a representative simulation, and six Chime animations (html/xyz, one for each of the MD trajectories) that can be easily visualized in one's favorite Internet navigator using the free Chemscape Chime plug-in (http://www.mdli.com/chemscape/chime/chime.html). This material is available free of charge via the Internet at http://pubs.acs.org.

JA042289G